Material tests with hull plating of MS Estonia

Investigation report

21.03.2024

Ordered by: Estonian Safety Investigation Bureau

Authors:

Mihkel Kõrgesaar, Professor in Naval Architecture, TalTech
Mart Saarna, Expert in mechanical testing, TalTech
Andrus Šults, Engineer, TalTech

Tallinn University of Technology, Kuressaare College

Telefon: 53439557

E-mail: mihkel.korgesaar@taltech.ee

Tallinna 19, Kuressaare

1 Introduction

The purpose of the work is to determine the mechanical material properties of two corroded steel plates. The geometry of the plates with the nominal sheet thickness is shown in Figure 1. The nominal sheet thickness was measured after rust removal, and this process is described in more detail in 2. The mechanical properties of the material were determined using tensile test specimens cut from the steel plates. Two different tests were performed: (1) a standard dog bone tensile test (hereinafter referred to as DB - dogbone) and (2) a notched tensile test specimen with the abbreviation NT (notched tension). The DB specimen was used to determine the stress-strain curve, while the material model was validated with the NT specimen. The specimens were laid on the steel plates in a way to obtain the maximum number of test specimens. The specimens were cut out of the plate at either 0 degrees (abbreviation L in the name of the specimen) or at an angle of 90 degrees (abbreviation T in the name of the specimen) to analyze the effect of the material orientation on the steel properties. During the experiment, the tensile force and the elongation of the specimen were recorded. Furthermore, in all experiments, a digital measuring system Aramis was used to record a video of the specimen surface during the experiment. In the analysis phase, the recording was used to determine the deformations and strains that occur in the specimens.

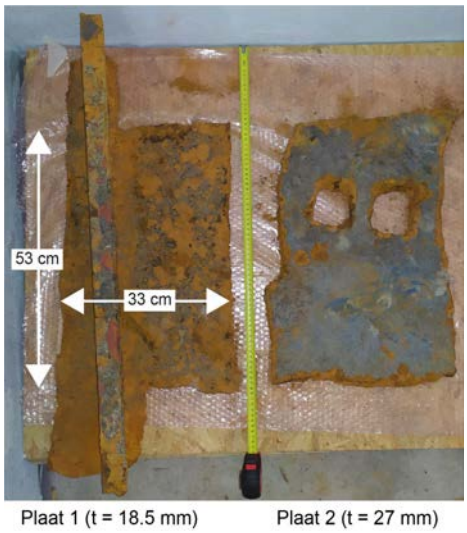

Figure 1: Corroded steel plates provided by the customer. Two plates are referenced throughout the report as indicated in the figure.

2 Experiments

2.1 Manufacturing of specimens

The outline of the cutting schema of the specimens is shown in Figure 2 (A). The specimens were cut out of the plate perpendicular to the surface of the plate with a band saw, and the final shape was achieved by milling. Thus, the nominal width of the specimens was the initial thickness of the steel plates (Figure 2 (B) and (C)). Figure 3 shows photographs of the specimens. Figure 3 (A) and (C) show the edges of the specimens after cleaning from loose rust and blue paint. The thickness of the plates (not the specimens) was measured after those procedures. After cleaning the thickness of Plate 1 was ∼18.5 mm and Plate 2 ∼27 mm.

The thickness of the specimens was chosen based on the recommendations of the standards for the shape of the deformable part of the DB specimen (length/width/thickness ratio). Thus, the nominal thickness of the cut specimens was obtained $t_1 = 6$ mm (Plate 1) and $t_2 = 10$ mm (Plate 2). To study the effect of the orientation of the material, the specimens were cut from the longitudinal (L) and transverse (T) direction of the plate, where the directions are determined according to the right-hand coordinate system in the center of Figure 2. The goal was to obtain 6 specimens per direction and specimen type. The entire test matrix is shown in 1. According to the customer's wishes, not all specimens were tested. These specimens are marked "Retain" in the Table and handed over to the customer along with the report.

Table 1: Test matrix with metadata.

Plate 1

Specimen name	cut	Test	Thickness (mm)	Width (mm)
P1_DB_T1	Yes	Yes	5.86	13.00
P1_DB_T2	Yes	Yes	5.81	13.01
P1_DB_T3	Yes	Yes	5.85	13.06
P1_DB_T4	Yes	Retain		
P1_DB_T5	Yes	Retain		
P1_DB_T6	Yes	Retain		
P1_DB_L1	Yes	Yes	5.85	13.01
P1_DB_L2	Yes	Yes	5.76	13.12
P1_DB_L3	Yes	Yes	5.92	13.08
P1_DB_L4	Yes	Retain		
P1_DB_L5	Yes	Retain		
P1_NT_T1	Yes	Yes	5.86	10.08
P1_NT_T2	Yes	Yes	5.67	10.01
P1_NT_T3	Yes	Yes	5.80	9.91
P1_NT_T4	Yes	Retain		
P1_NT_T5	Yes	Retain		
P1_NT_T6	Yes	Retain		
P1_NT_L1	Yes	Yes	5.74	9.70
P1_NT_L2	Yes	Yes	5.65	8.75
P1_NT_L3	Yes	Yes	6.01	8.87
P1_NT_L4	Yes	Retain		
P1_NT_L5	Yes	Retain		
P1_NT_L6	Yes	Retain	Production defect	
P1_NT_L7	Yes	Retain	Production defect	

Plate 2

Specimen name	cut	Test	Thickness (mm)	Width (mm)
P2_DB_L1	Yes	Yes	10,13	20
P2_DB_L2	Yes	Yes	10,14	20
P2_DB_L3	Yes	Yes	10,12	20
P2_DB_L4	Yes	Retain	10	
P2_DB_L5	Yes	Retain	10	
P2_DB_L6	Yes	Retain	10	
P2_DB_T1	Yes	Yes	10,15	20
P2_DB_T2	Yes	Yes	10,15	20
P2_DB_T3	Yes	Retain	10	
P2_DB_T4	Yes	Retain	10	
P2_NT_T1	Yes	Yes	10	10
P2_NT_T2	Yes	Yes	10	10
P2_NT_T3	Yes	Yes	10	10
P2_NT_T4	Yes	Retain	10	
P2_NT_T5	Yes	Retain	10	
P2_NT_T6	Yes	Retain	10	
P2_NT_L1	Yes	Yes	10	10
P2_NT_L2	Yes	Yes	10	10
P2_NT_L3	Yes	Yes	10	10
P2_NT_L4	Yes	Retain	10	
P2_NT_L5	Yes	Retain	10	
P2_NT_L6	Yes	Retain	10	

DB specimens test speed 1 = 0,75 mm/min (until 0,8 %). Test speed 2 was 15 mm/min (until fracture)
NT specimens with test speed of 5 mm/min

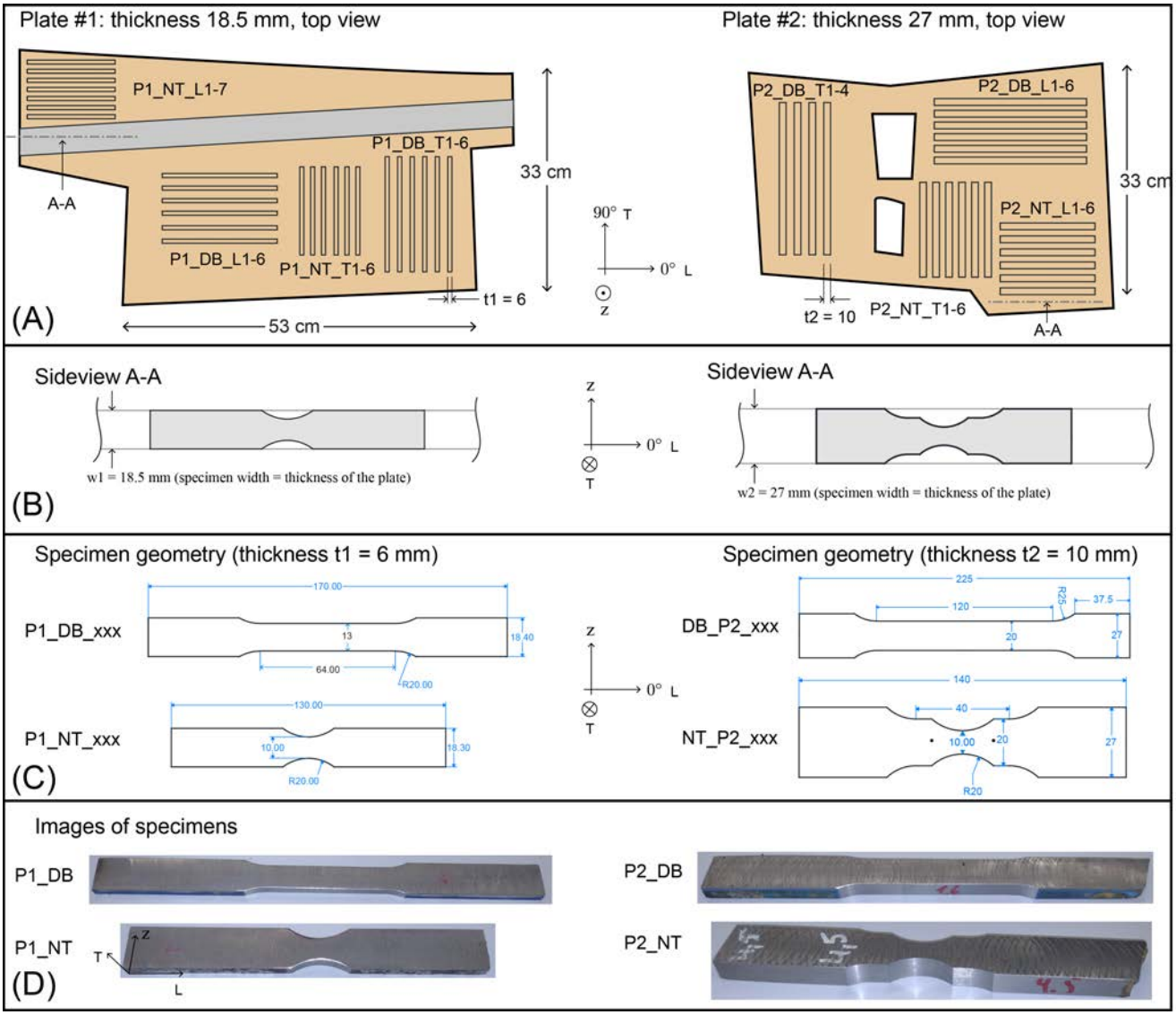

Figure 2: Geometry and cutting scheme of the specimens. Plate 1 on the left, plate 2 on the right.

2.2 Conducting the tests

Since the goal was to determine the static strength properties of the material, the experiments were carried out at low speeds. The chosen testing speed in table 1 was based on the experience of the laboratory technicians and literature, e.g [1]. The parameters of the Aramis system used for the measurement are shown in Table 2. During the experiments, the following information was recorded. The Instron tensile test machine recorded the tensile force. The corresponding elongation of the specimen was measured using an extensometer glued to the specimen. Furthermore, the entire test run was recorded using Aramis Digital Image Correlation system, which means that pictures were taken of the entire test specimen with a frequency of 15 Hz.

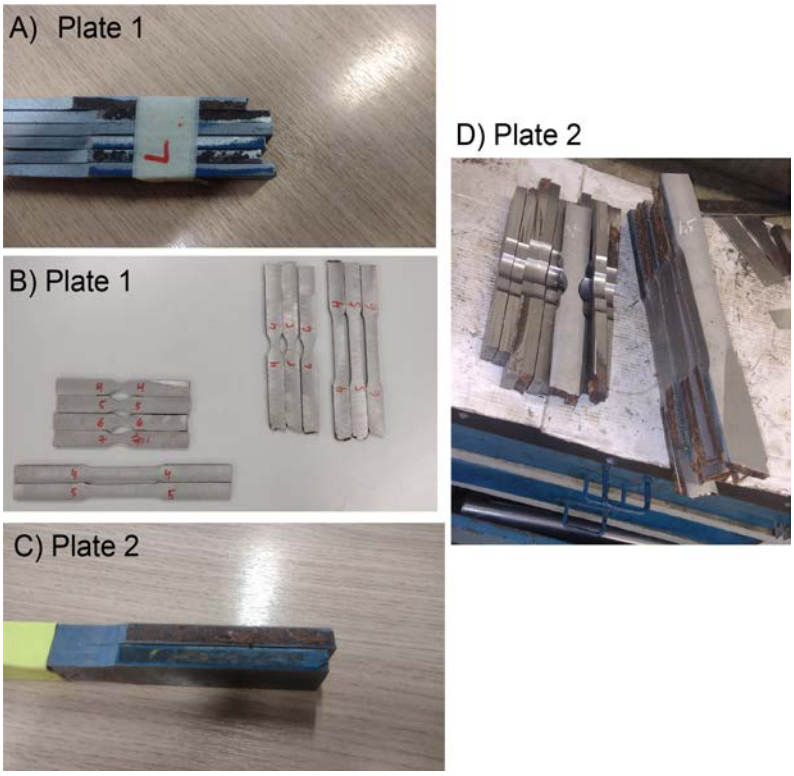

Figure 3: Cut specimens.

Table 2: Aramis system parameters during the tests

DIC method:	Aramis 3D Stereo image surface measurement
Camera type / Lens:	12MP / 50 mm
Measuring vol. / dist.:	MVO (L:175 x W:130 x D:110) / 696 mm
Calibration obj. / deviation:	CP40/170/43505 / 0.03001
Facet size [px]	19
Step size [px]	16
Strain window [nr]	1
Pixel size [mm]	0.0425
Calc. strain ref. length (mm)	0.8075 = (Strain window− 1)· Step size+ Facet size
Tensile test method:	EN6892-1 (loading speed slightly different because of DIC)
Tensile test equipment:	Plaat 1: Instron 8516 (100 kN), Plaat 2: Instron 8802 (250 kN)
Tesnsile test operator:	Mart Saarna

2.3 Test results

For each test, an excel file containing various determined characteristics is obtained. The most important of this information, such as the material yield stress σ_0, the length of the virtual extensometer L_0, the elongation of the virtual extensometer ΔL, and the corresponding measured force F were used to determine the true stress-strain curve.

3 Analysis

The same methodology was used to determine the material's true stress-strain curve for both plates. Therefore, this chapter presents the general principle of the method, which was applied to both plates.

Initially, the nominal strength properties of the material were found, i.e. an engineering stress-strain curve of the material ($\sigma_{eng} - \varepsilon_{eng}$). For this purpose, DB test specimens were used. The engineering stress σ_{eng} was determined as the ratio of the measured force F to the initial cross-sectional area of the specimen A_0.

$$\sigma_{eng} = \frac{F}{A_0}. \tag{1}$$

Engineering strain ε_{eng} was found using equation

$$\varepsilon_{eng} = \frac{\Delta L}{L_0}, \tag{2}$$

where ΔL is the elongation of the specimen and $L_0 = 50$ mm is the initial length of the virtual extensometer. The engineering stress-strain curve primarily describes the properties of the specimen. To characterize the material itself the true stress-strain curve $\sigma_T - \varepsilon_p$ is used. Until necking, this relationship can be determined on the basis of nominal values using the following equations

$$\sigma_T = \sigma_{eng}(1 + \epsilon_{eng}) \tag{3a}$$

$$\varepsilon_p = \log(1 + \varepsilon_{eng}) \tag{3b}$$

The beginning of the neck formation coincides with the maximum force and the value of the maximum engineering stress, since when necking occurs, the cross-sectional area begins to decrease. However, the actual true stress in the material increases. Since it is very difficult to measure the true cross-sectional area in practice, the equation(2)cannot be used to determine the true stress. Therefore, the three-step method described in [2] and [3] was used to determine $\sigma_T - \varepsilon_T$.

In the first step a mathematical model is created, which can describe the true stress-strain relation of the steel. The model is combined from two well-known equations often used to describe the true stress-strain curve of metals. These are the Voce model and the Swift model:

$$\sigma_{T-Voce} = \sigma_0 + Q(1 - e^{-C_1 \varepsilon_p}) \tag{4a}$$

$$\sigma_{T_Swift} = A\left(\varepsilon_p + \varepsilon_0\right)^n \tag{4b}$$

where coefficients Q, C_1, A,ε_{plat} and n are variables that need to be specified and ε_0 is a parameter that is found as follows

$$\varepsilon_0 = \left(\frac{\sigma_0}{A}\right)^{(1/n) - \varepsilon_{plat}} \tag{5}$$

The material is described as a linear combination of these two models as follows:

$$\sigma_{T-Voce} = (1-\alpha)\sigma_{T-VOCE} + \alpha\sigma_{T-Swift} \tag{6}$$

where α is the weight coefficient, which must be determined. Once the corresponding coefficients and variables have been found, the material can be described using the equation (6) and used in LEM simulations.

In **Step two** of the method, the coefficients of the model are determined through optimization by minimizing the value Ψ, which characterizes the residual of the measured true stress (determined by the formula (3a) and the true stress of the model σ_{T-Voce}

$$\psi[\alpha] = \sum_{i=1}^{Np} \left(\sigma^{i}_{T-Voce-mudel}[\alpha] - \sigma^{i}_{T-Aramis}\right)^2 \tag{7}$$

where i corresponds to a specific time instance, and N_p indicates the number of points that have been used in the optimization (these are shown in Figure 4(B) with a red marker).

In the third step the material model is validated. Validation is necessary because the optimization performed in Step 2 considered the experimentally measured points only up to the neck formation. At large deformations, the found model may be inaccurate. Numerical simulations with NT specimens were used for validation. Based on the symmetry of the specimen geometry, a 1/8 model of the NT specimen was created. The material model found in step 2 is used as the input material in simulations.

The simulation is carried out under the same conditions as the experiment. As a result of the simulation, a graph of force and deformation is obtained, which is compared to the experimentally measured values. If the simulation and test results differ, the material model does not correspond to reality. Consequently, material model parameters are slightly adjusted until sufficient similarity between the simulation and the test is achieved. The material model that leads to good correspondence between simulated and tested force-displacement relation is given to the customer.

4 Results

The results obtained using the methodology described in Section 3 are shown in Figure 4. Figure 4 shows the results of Plate 1 on the left and the results of Plate 2 on the right. Figure 4 (A) shows the measurement results and plots of the true stress-strain calculated using the equation (3). For both plates, the differences between the individual specimens are quite minimal, but more noticeable in the case of plate 1. The effect of the material orientation on the stress-strain curves is negligible, meaning that material is assumed to be isotropic. This is rather common for structural steels.

The yield stress of Plate 1 is $\sigma_0 = 245$ MPa and the yield stress of Plate 2 is $\sigma_0 = 294$ MPa. These results, along with other specified parameters are compiled in Table 3. Inserting the given values into the model (equations 4-6), we obtain the stress-strain curves (in black) shown in Figure 4 (B). These curves have been validated by FEM simulations (NT specimens) as shown in Figure 4 (C). In simulations a virtual extensometer with a same length as used in experiments of (30 mm) has been used.

Table 3: Material model properties for both plates.

	Plaat 1	Plaat 2	
σ_0	245	294	MPa
ε_{plat}	0.02	0.02	
n	0.26	0.26	
A	1050	1050	MPa
Q	200	200	MPa
C_1	11.2116	11.2116	
α	0.3762	0.4492	
ε_0	-0.01629	-0.01252	

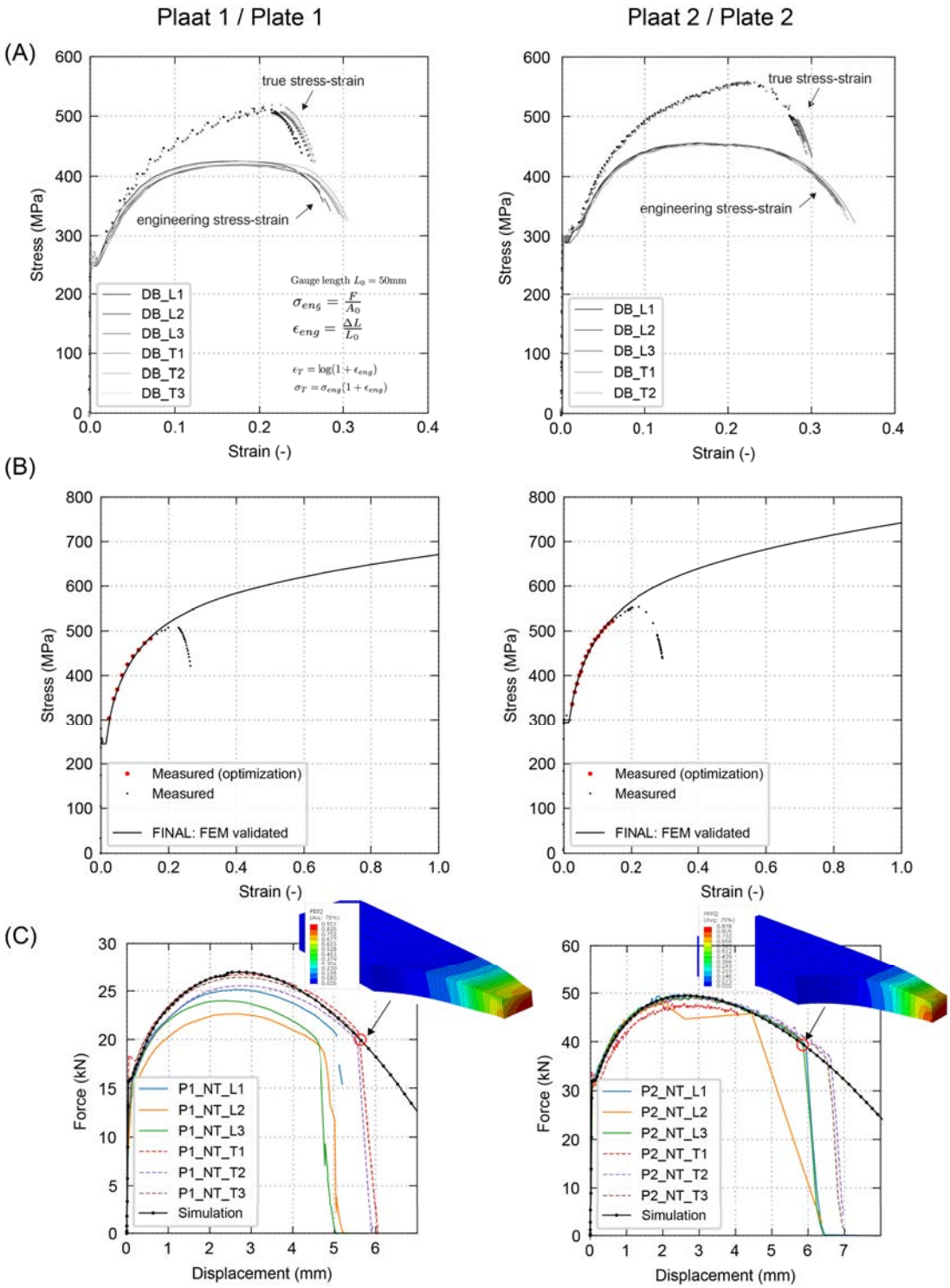

Figure 4: A) Engineering stress-strain curves. B) Determined true stress-strain cuves. C) Validation with an NT specimen.

Figure 5 (A) shows the von Mises strains measured by Aramis on DB specimens (L-directional) at the moment before fracture onset. In each specimen the highest von Mises strains are highlighted. The Aramis results displayed in image (A), can optionally be plotted later for each deformation state using the script /Analyses/Experimental/Surface_strain_at_specific_stage.ipynb. For illustrative purposes, the script above is used to plot the von Mises equivalent strain in Figure 5 (B) for the specimen P1_DB_L1 at the same instance as in Figure 5 (A). Thus, the script enable to either examine or further analyze the deformations later if desired.

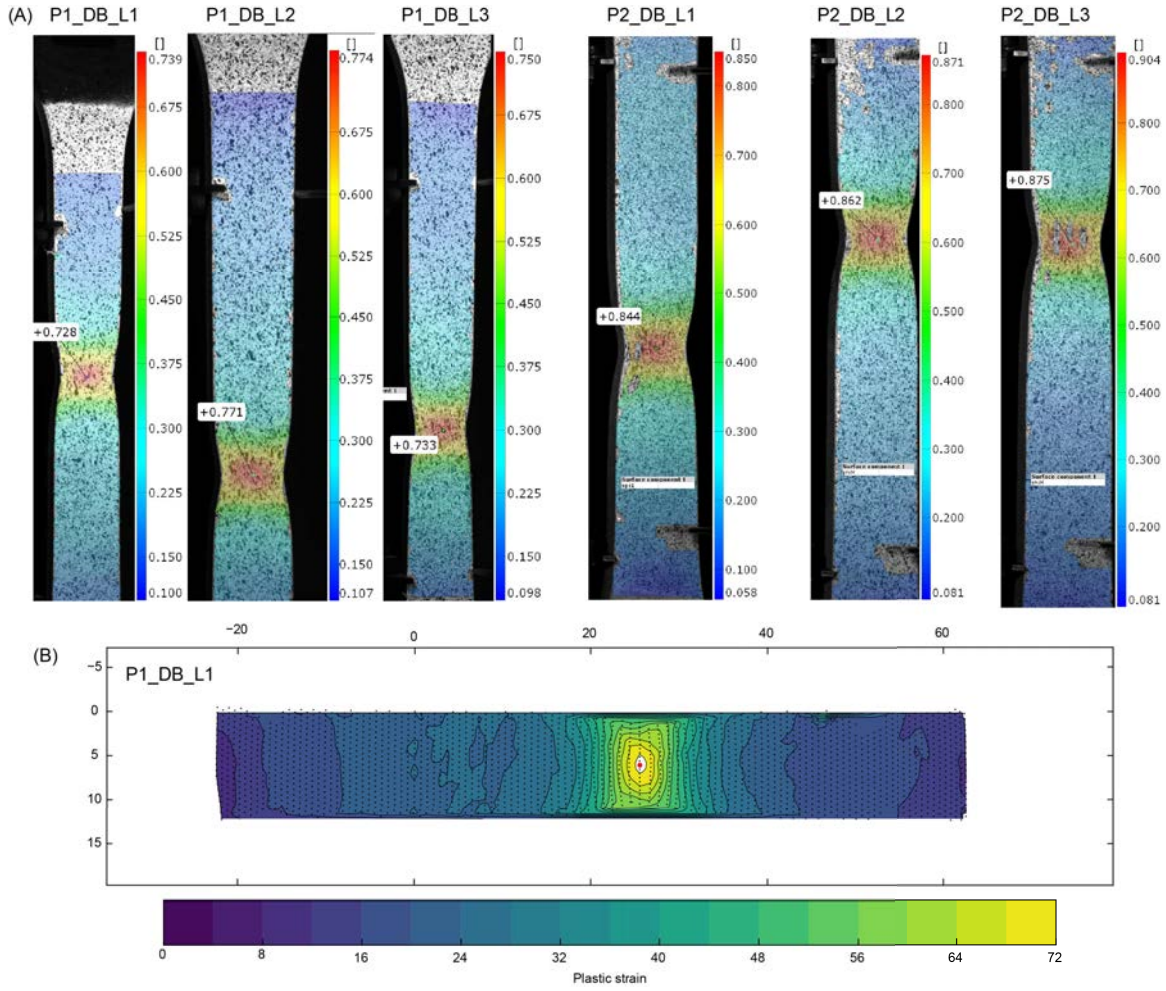

Figure 5: (A) von Mises deformations on the surface of the DB specimen before fracture. (B) Aramis DIC results of test P1_DB_L1 at the same time instance as shown in Figure A.

Figure 6 displays the resulting material curves in comparison with the material curves used in the seabed contact simulations in LS-DYNA with ferry Estonia. The differences between the curves are quite large, with the actual material being stronger than the material used in the simulations. Such a significant difference is also likely to affect the results of the simulations. Using the measured material curves in the ferry simulations in this report, the extent of the deformations should decrease compared to the initial simulations. Given the differences in

curves, it is recommended to repeat the ferry simulations with new material curves.

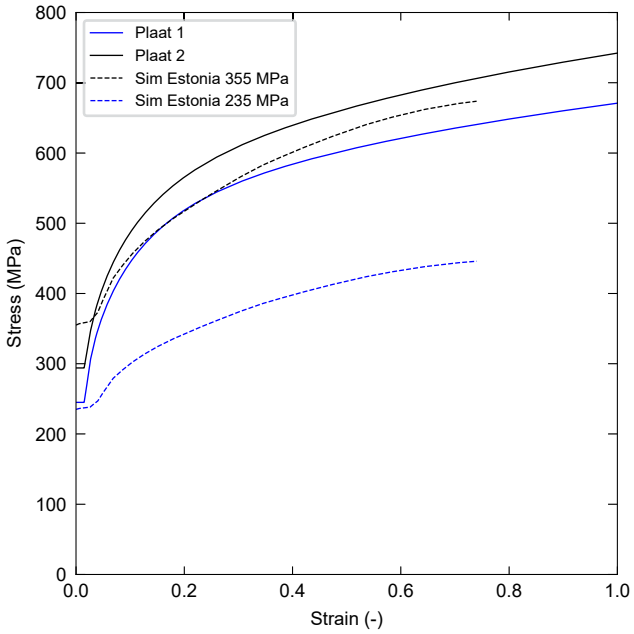

Figure 6: Comparison of the material curves.

APPENDIX 1
The origin of the hull plating cutouts (material samples) of MV Estonia

During the marine works commissioned by the Swedish Maritime Administration (*Sjöfartsverket*) in early December 1994, among other tasks, divers cut two openings in the port side of the wreck of MV Estonia to access the interior of the wreck. Due to the fender line and the minimal inclination of the hull in these areas, some of the steel plates from the cutouts of both openings remained on the port side of the wreck near the openings. In July 2023, during marine works commissioned by the Swedish Accident Investigation Board (*Statens haverikommission*), from both openings one steel plate was recovered.

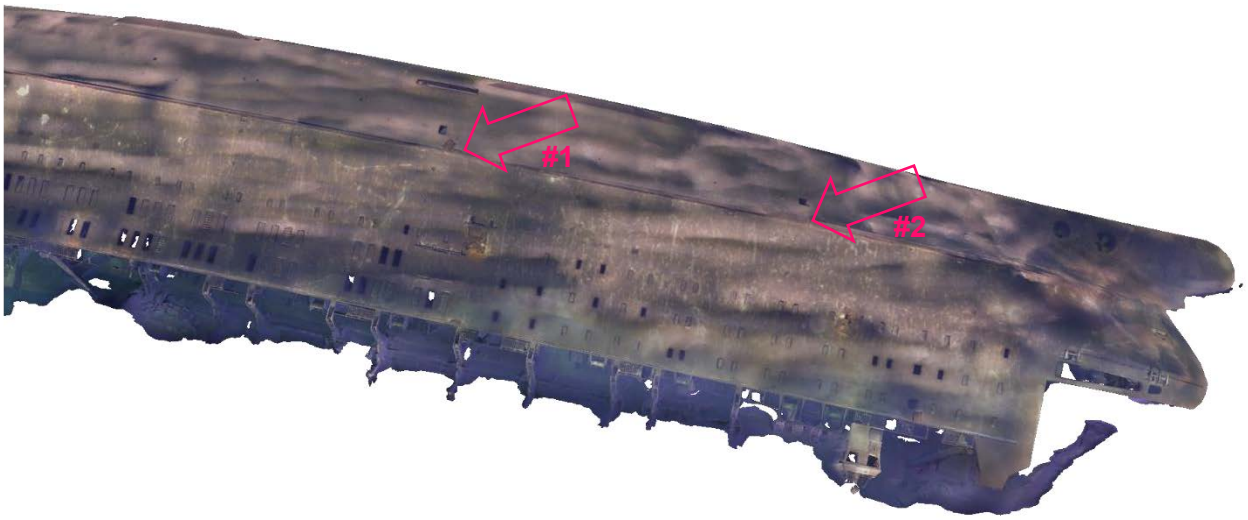

Figure 1. Locations of steel plates (#1 and #2) on the port side of the photogrammetric model (2022) of the wreck of MV Estonia during the years 1994-2023. Source: Estonian Safety Investigation Bureau

Figure 2. Opening in the midships cut by the divers (on the left), shifted cover grating of the opening (at the centre), and steel plate #1 (in right) on the photogrammetric model of the wreck (2022). Source: Estonian Safety Investigation Bureau

Figure 3. Forward opening cut by the divers (on the left) and steel plate #2 (on the right) on the photogrammetric model of the wreck (2022). Source: Estonian Safety Investigation Bureau

Figure 4. Recovered steel plates from the wreck of MV Estonia on the deck of the research vessel Viking Reach on July 21, 2023. Source: Tauri Roosipuu, Estonian Safety Investigation Bureau

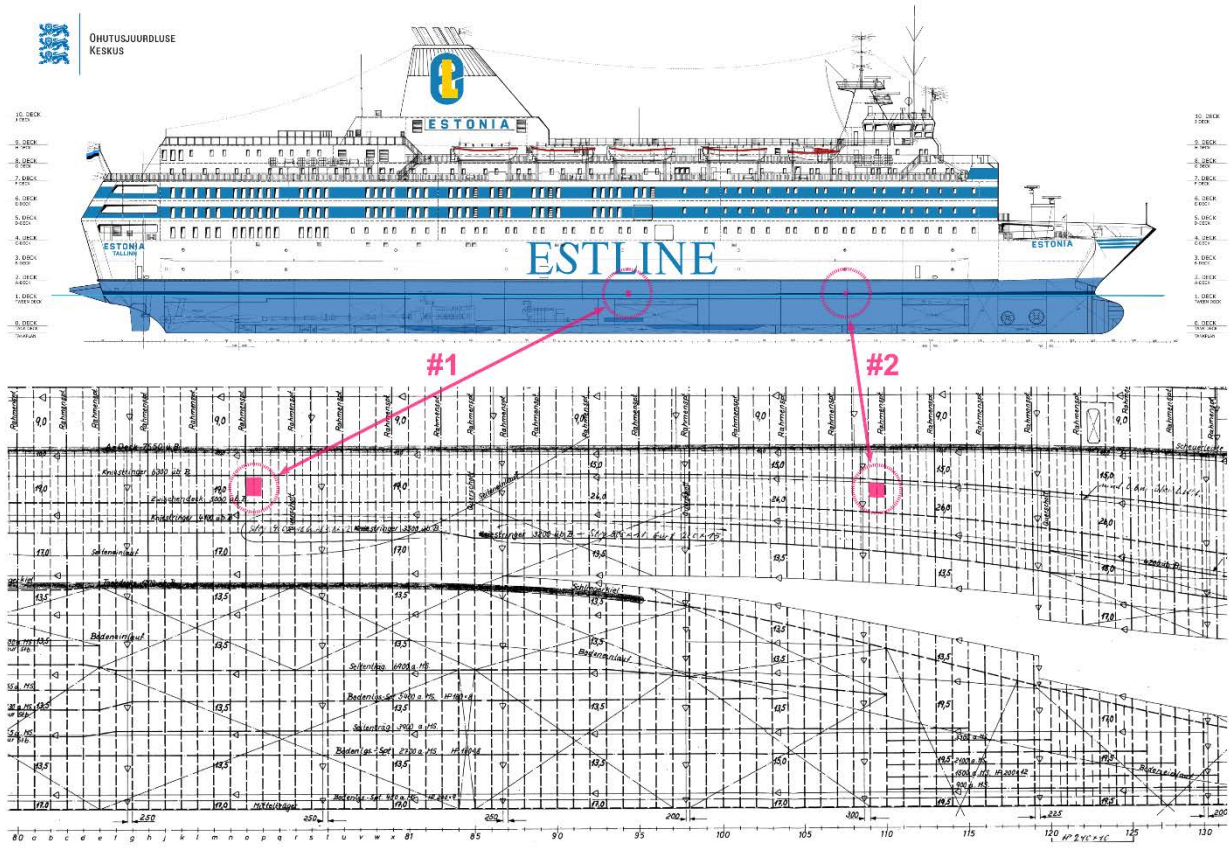

Figure 3. Locations of the hull plating cutouts (#1 and #2) on the general arrangement plan of MV Estonia (on the top) and on the shell plating drawing (on the bottom, 1003 Außenhautabwicklung, 30.01.1980 [G]). Steel plate #1 origins from near the waterline between frames o and p, and according to the drawing, the thickness of the hull plating in this area is 19.0 mm. Steel plate #2 origins from near the waterline between frames 109 and 110, located at the upper edge of the ice belt, and according to the drawing, the thickness of the hull plating in this area is 26.0 mm. Source: Estonian Safety Investigation Bureau

APPENDIX 2

The files included with the report are briefly described in the Table 4.

Table 4: Attached files and a brief descritpion of their content.

Plaat 1	
Folder: Tellijale\Experimental\Plaat1-DB	
Summary_data_P1_DB_L1.xlsx	Data in multiple sheets. Summary, Fracture_section_data, History_data, Section_y_data, Material instron, Aram
Summary_data_P1_DB_L2.xlsx	Data in multiple sheets. Summary, Fracture_section_data, History_data, Section_y_data, Material instron, Aram
Summary_data_P1_DB_L3.xlsx	Data in multiple sheets. Summary, Fracture_section_data, History_data, Section_y_data, Material instron, Aram
Summary_data_P1_DB_T1.xlsx	Data in multiple sheets. Summary, Fracture_section_data, History_data, Section_y_data, Material instron, Aram
Summary_data_P1_DB_T2.xlsx	Data in multiple sheets. Summary, Fracture_section_data, History_data, Section_y_data, Material instron, Aram
Summary_data_P1_DB_T3.xlsx	Data in multiple sheets. Summary, Fracture_section_data, History_data, Section_y_data, Material instron, Aram
Coordinate_P1_DB_L1.npy,eps_vm_P1_DB_L1.npy	
Coordinate_P1_DB_L2.npy,eps_vm_P1_DB_L2.npy	
Coordinate_P1_DB_L3.npy,eps_vm_P1_DB_L3.npy	Equivalent plastic strain throught experiment
Coordinate_P1_DB_T1.npy,eps_vm_P1_DB_T1.npy	
Coordinate_P1_DB_T2.npy,eps_vm_P1_DB_T2.npy	
Coordinate_P1_DB_T3.npy,eps_vm_P1_DB_T3.npy	
Folder: Tellijale\Experimental\Plaat1-NT	
P1_NT_L1_Extenso_30.csv	Colon separated info of: index, delta L, delta L %, Load
P1_NT_L2_Extenso_30.csv	Colon separated info of: index, delta L, delta L %, Load
P1_NT_L3_Extenso_30.csv	Colon separated info of: index, delta L, delta L %, Load
P1_NT_T1_Extenso_30.csv	Colon separated info of: index, delta L, delta L %, Load
P1_NT_T2_Extenso_30.csv	Colon separated info of: index, delta L, delta L %, Load
P1_NT_T3_Extenso_30.csv	Colon separated info of: index, delta L, delta L %, Load
Coordinate_P1_NT_L1.npy, eps_vm_P1_NT_L1.npy	
Coordinate_P1_NT_L2.npy, eps_vm_P1_NT_L2.npy	
Coordinate_P1_NT_L3.npy, eps_vm_P1_NT_L3.npy	Equivalent plastic strain throught experiment
Coordinate_P1_NT_T1.npy, eps_vm_P1_NT_T1.npy	
Coordinate_P1_NT_T2.npy, eps_vm_P1_NT_T2.npy	
Coordinate_P1_NT_T3.npy, eps_vm_P1_NT_T3.npy	
Plaat 2	
Folder: Tellijale\Experimental\Plaat2-DB	
Summary_data_DB_L1.xlsx	Data in multiple sheets. Summary, Fracture_section_data, History_data, Section_y_data, Material instron, Aram
Summary_data_DB_L2.xlsx	Data in multiple sheets. Summary, Fracture_section_data, History_data, Section_y_data, Material instron, Aram
Summary_data_DB_L3.xlsx	Data in multiple sheets. Summary, Fracture_section_data, History_data, Section_y_data, Material instron, Aram
Summary_data_DB_T1.xlsx	Data in multiple sheets. Summary, Fracture_section_data, History_data, Section_y_data, Material instron, Aram
Summary_data_DB_T2.xlsx	Data in multiple sheets. Summary, Fracture_section_data, History_data, Section_y_data, Material instron, Aram
Coordinate_P2_DB_L1.npy, eps_vm_P2_DB_L1.npy	
Coordinate_P2_DB_L2.npy, eps_vm_P2_DB_L2.npy	
Coordinate_P2_DB_L3.npy, eps_vm_P2_DB_L3.npy	Equivalent plastic strain throught experiment
Coordinate_P2_DB_T1.npy, eps_vm_P2_DB_T1.npy	
Coordinate_P2_DB_T2.npy, eps_vm_P2_DB_T2.npy	
Folder: Tellijale\Experimental\Plaat2-DB	
P2_NT_L1_Extenso_30.csv	Colon separated info of: index, delta L, delta L %, Load
P2_NT_L2_Extenso_30.csv	Colon separated info of: index, delta L, delta L %, Load
P2_NT_L3_Extenso_30.csv	Colon separated info of: index, delta L, delta L %, Load
P2_NT_T1_Extenso_30.csv	Colon separated info of: index, delta L, delta L %, Load
P2_NT_T2_Extenso_30.csv	Colon separated info of: index, delta L, delta L %, Load
P2_NT_T3_Extenso_30.csv	Colon separated info of: index, delta L, delta L %, Load
Coordinate_P2_NT_L2.npy, eps_vm_P2_NT_L2.npy	
Coordinate_P2_NT_L3.npy, eps_vm_P2_NT_L3.npy	
Coordinate_P2_NT_T1.npy, eps_vm_P2_NT_T1.npy	Equivalent plastic strain throught experiment
Coordinate_P2_NT_T2.npy, eps_vm_P2_NT_T2.npy	
Coordinate_P2_NT_T3.npy, eps_vm_P2_NT_T3.npy	
True stress strain curves	
Folder: Tellijale	
Materjal-plaat1-sim-NT-MAT1-SIMTEST3.inp	True stress strain together with model parameters for plate 1
Materjal-plaat2-sim-NT-MAT2-SIMTEST5.inp	True stress strain together with model parameters for plate 2

References

[1] C. C. Roth and D. Mohr, "Effect of strain rate on ductile fracture initiation in advanced high strength steel sheets: Experiments and modeling," *International Journal of Plasticity*, vol. 56, pp. 19–44, 2014.

[2] J. H. Sung, J. H. Kim, and R. Wagoner, "A plastic constitutive equation incorporating strain, strain-rate, and temperature," *International Journal of Plasticity*, vol. 26, no. 12, pp. 1746–1771, 2010.

[3] D. Mohr and S. J. Marcadet, "Micromechanically-motivated phenomenological hosford-coulomb model for predicting ductile fracture initiation at low stress triaxialities," *International Journal of Solids and Structures*, vol. 67-68, pp. 40–55, 2015.